



## CORRECTION OF FLUX ERROR IN LOW SPEED RANGE OF DTC DRIVES OF INDUCTION MACHINES

Mohsen Dashtbani<sup>1</sup>, Majid Hasan zadeh<sup>1</sup>, Reza Roshanfekar<sup>1\*</sup>

### Abstract

The conventional direct torque control (DTC) method suffers a flux drop at low speeds, which is due to the long selection of zero (neutral) voltage vectors in these speed areas. Past studies with the continuous switch of direct and reverse active vectors to achieve proper flux adjustment, this procedure causes high and consecutive overshoots in the hysteresis band that causes a sharp increase in the switching frequency and increase in the torque and current ripple, which means decrease in the drive efficiency. In this article, a modified method for setting the standard DTC current is introduced, which can be achieved by controlling only one band (low or high band) at low speeds. The introduced method by reducing the selection of zero voltage vectors and at the same time minimizing the number of reverse voltage vectors prevents the loss of flux in low speed areas. In addition, it is effective in reducing torque ripple and current in low speed mode and a significant reduction in switching frequency will also be achieved. The effectiveness of the proposed method in the simulation which is done in MATLAB software will be proved.

**Keywords:** Direct torque control, flux adjustment, induction motor.

*Received Date: 2023-05-10; Revised Date: 2023-06-12; Accepted Date: 2023-08-23.*

## 1. INTRODUCTION

Asynchronous (induction) motors have been used since about a hundred years ago due to advantages such as no complicated structure, high power, good reliability, more reasonable price, low volume and weight. Among the advantages of asynchronous motors compared to DC motors are size, weight and less rotor inertia, higher efficiency, better stability, lower cost, less maintenance and easier maintenance than DC motors [1, 2]. There are various methods to control the drive of induction motors, which is called variable frequency drive (VFD). VFD can be without sensors or with sensors. Controllers with sensors are scalar controllers and vector controllers. Vector controllers are mainly called field oriented control (FOC) and direct torque control (DTC), which each has its advantages and disadvantages [3]. Figure 1 shows the classification chart for control strategies and Table 1 shows their advantages and disadvantages.

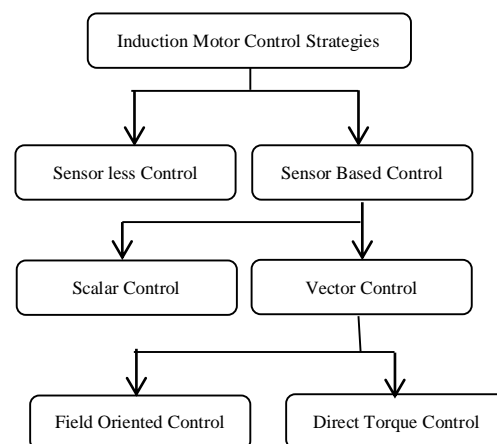


**Fig. 1.** CLASSIFICATION OF INDUCTION MOTOR CONTROL STRATEGIES

<sup>1</sup>Hakim Sabzevari university, sabzevar

\*Corresponding author, Email: r.roshanfekar@hsu.ac.ir

@ 2022 Niroo Research Institute, All rights reserved.

TABLE 1. CLASSIFICATION OF INDUCTION MOTOR CUSTOMARY CONTROL STRATEGIES

Control strategy		Advantages	Disadvantages	
Sensor-less		<ul style="list-style-type: none"> <li>• Low cost</li> <li>• High reliability</li> <li>• Less maintenance requirements [4]</li> </ul>	<ul style="list-style-type: none"> <li>• Low speed capacity</li> <li>• Low speed accuracy</li> <li>• Low speed range generation instability [4]</li> </ul>	
Sensor based	Scalar	<ul style="list-style-type: none"> <li>• Low cost</li> <li>• Simplicity</li> <li>• Immunity to errors of feedback signals [5]</li> </ul>	<ul style="list-style-type: none"> <li>• Uncontrollable torque</li> <li>• Used in minimum motor performance [5]</li> </ul>	
	Vector	FOC	<ul style="list-style-type: none"> <li>• Implemented more efficiency</li> <li>• More processing power [6]</li> </ul>	<ul style="list-style-type: none"> <li>• PI parameters are difficult to set</li> <li>• Current dynamic response is slow [6]</li> </ul>
		DTC	<ul style="list-style-type: none"> <li>• Torque and flux can be changed very fast by changing the references</li> <li>• High efficiency</li> <li>• Low losses</li> <li>• No overshoot in step response [6]</li> </ul>	<ul style="list-style-type: none"> <li>• High flux and torque ripples specially at low speed regions [6]</li> </ul>

One of these modern methods of driving induction motors is called DTC [2]. In this method, by using the feedback signals obtained from the current and voltage of the stator of the induction motor and by modeling the operation of the motor, the torque and linkage flux of the motor are estimated and based on the error of the flux and torque of the motor, appropriate switching commands are applied to the inverter. Therefore, the torque and stator current of the induction motor will be controlled, and the appropriate speed control will be created [2]. Advantages such as convenient implementation, fast dynamic response and lack of dependence on motor parameters have caused this control method to attract a lot of attention in the research community. classical DTC strategy suffers from high torque ripple, flux drop in low speed, and very fast sampling time and introduce a method to overcome these flaws can be very valuable [7]. Various methods have been introduced in order to improve the performance of the DTC method in the drive of induction motors. Some of these methods are increasing the number of state vectors, using three-level inverters instead of two levels, DTC is based on multi-level inverters [8, 9] a common method is integration of SVM with DTC under the title of DTC-SVM [10]. Most of these methods solve the basic defects of the classical DTC method to an acceptable extent, but they greatly increase the computational load of the system and make the structure of the drive complicated, and for

its implementation, it is necessary to know the parameters of the motor at any moment. Therefore, introducing a method that can improve the defects of the classic DTC method while being simple and independent of the parameters of the motor is of great importance.

In the next section, the details of the DTC method are described, including the general structure, equations, switching tables and vectors figures. In the later section, the method of calculating the reference flux and torque is presented, and the proposed method for setting the desired flux value is presented. Finally, the parameters of the induction motor and the simulation of the proposed method is present, and the simulation results are presented in comparison with results of two other methods to adjust the flux at low speeds.

## 2. CONTROL OF INDUCTION MOTORS BY DTC METHOD

The general schematic of direct torque control of induction motors is Fig. 2:

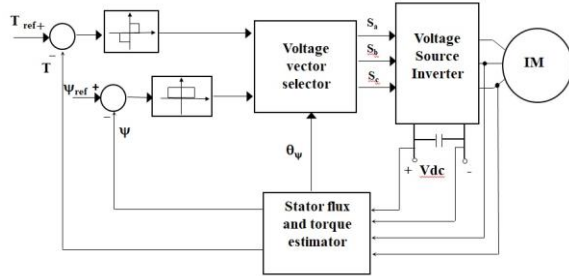


Fig. 2. SCHEMATIC OF DIRECT TORQUE CONTROL OF INDUCTION MOTORS

The hysteresis controller in the direct torque method generates torque and flux error status. Based on these error states and the stator flux angle vector in order to maintain the torque error and the stator flux within the hysteresis band will be choose [11]. The required control voltage vector is selected as shown in Table 2:

TABLE 2. DTC METHOD SWITCH TABLE IN ORDER TO MAINTAIN THE TORQUE AND STATOR FLUX ERROR WITHIN THE HYSTERESIS BAND

stator		1	2	3	4	5	6
flux	torque						
$\Delta\psi=1$	$\Delta T=1$	$V_2$	$V_3$	$V_4$	$V_5$	$V_6$	$V_1$
	$\Delta T=0$	$V_7$	$V_0$	$V_7$	$V_0$	$V_7$	$V_0$
	$\Delta T=-1$	$V_6$	$V_1$	$V_2$	$V_3$	$V_4$	$V_5$
$\Delta\psi=0$	$\Delta T=1$	$V_3$	$V_4$	$V_5$	$V_6$	$V_1$	$V_2$
	$\Delta T=0$	$V_0$	$V_7$	$V_0$	$V_7$	$V_0$	$V_7$
	$\Delta T=-1$	$V_5$	$V_6$	$V_1$	$V_2$	$V_3$	$V_4$

The structure of a 2-level voltage source inverter (VSI) used in DTC drives is shown in Fig. 3.

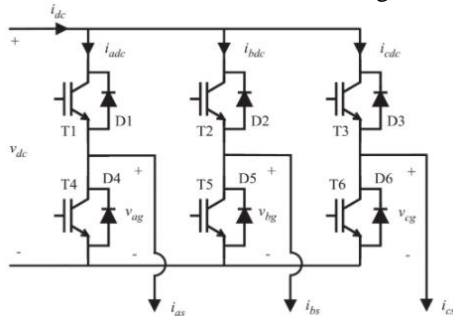


Fig. 3. THE STRUCTURE OF A 2-LEVEL VOLTAGE INVERTER USED IN INDUCTION MOTOR DTC DRIVES

The important thing about this 2-level inverter is that two switches that exist in the same leg cannot be activated at the same time because it causes a short circuit of the source [12]. The Table 3 shows the different modes for the switches.

TABLE 3. DIFFERENT SWITCH STATES TO CREATE DIFFERENT VOLTAGE VECTORS

Voltage Vector	$T_1/T_4$	$T_2/T_5$	$T_3/T_6$
$V_0$	0	0	0
$V_1$	1	0	0
$V_2$	1	1	0
$V_3$	0	1	0
$V_4$	0	1	1
$V_5$	0	0	1
$V_6$	1	0	1
$V_7$	1	1	1

The state vector when all switches are inactive ( $V_0$ ) and the state vector when all switches are active ( $V_7$ ) are called zero or neutral voltage vector. The other remained situations are the active or main vectors whose absolute magnitude is  $2/3$  of the DC link voltage.

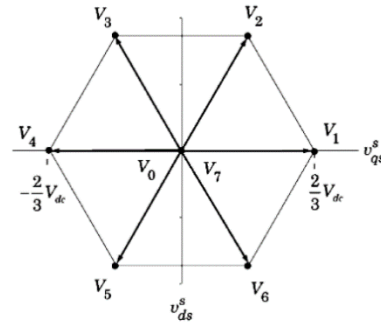
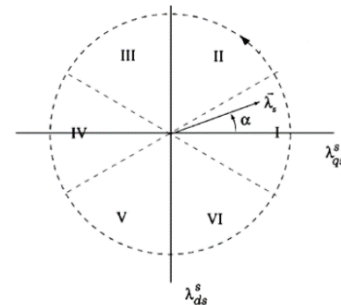


Fig. 4. DIFFERENT INVERTER OUTPUT VOLTAGE VECTORS

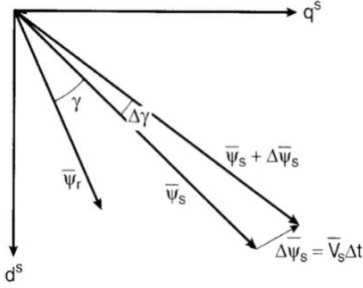
According to the 6 active vectors, the voltage vector plane is divided into 6 parts, each of which is named with its own vector. Figure 5 shows this zoning.



**Fig. 5. ZONING OF INVERTER VOLTAGE VECTORS**

Each vector is located exactly in the center of its respective area. Now that we have fully understood the structure of the inverter, we will discuss how to directly control the torque.

The electromagnetic torque relationship in terms of rotor flux and stator flux can be expressed as follows:


**Fig. 6. DISPLAY FLUX VECTORS ON DQ PAGE**

$$T_e = \frac{3}{2} p \frac{L_m}{\sigma L_s L_r} |\vec{\psi}_s| |\vec{\psi}_r| \sin \gamma \quad (1)$$

$$\vec{\psi}_s (= [\psi_{sd} \ \psi_{sq}]^T) \quad (2)$$

$$\vec{\psi}_r (= [\psi_{rd} \ \psi_{rq}]^T) \quad (3)$$

$\vec{\psi}_s$  is stator flux vector and  $\vec{\psi}_r$  is rotor flux vector  
 $\omega_r$  is the rotor speed of the electrical motor in radians per second. P is the even number of motor poles, and  $\gamma$  is the load angle between the stator and rotor shafts.

$$\sigma = 1 - \frac{L_m^2}{L_s L_r} \quad (4)$$

$$0 = R_r \cdot \vec{i}_r - j\omega_r \cdot \vec{\psi}_r + \frac{d\vec{\psi}_r}{dt} \quad (5)$$

$$\vec{\psi}_s = L_s \cdot \vec{i}_s + L_m \cdot \vec{i}_r \quad (6)$$

$$\vec{\psi}_r = L_r \cdot \vec{i}_r + L_m \cdot \vec{i}_s \quad (7)$$

Equation (8) shows the relationship between stator flux and stator voltage.

$$\vec{v}_s = R_s \cdot \vec{i}_s + \frac{d\vec{\psi}_s}{dt} \quad (8)$$

If we ignore the stator ohmic voltage drop

$$\frac{d\vec{\psi}_s}{dt} = \vec{v}_s - R_s \cdot \vec{i}_s \approx \vec{v}_s \quad (9)$$

Therefore, in a very small-time slice, flux changes are equal to voltage. Also, if we want to write the rotor flux in terms of the stator flux:

$$\frac{d\psi_r}{dt} + \left( \frac{L_m}{\sigma L_s L_r} - \frac{R_r}{L_r} - j\omega_{sl} \right) \psi_r = R_r \frac{L_m}{\sigma L_s L_r} \psi_s \quad (10)$$

In the aforementioned equations,  $R_s$  and  $R_r$  are stator resistance and rotor resistance respectively, and  $L_s$  and  $L_r$  and  $L_m$  are stator inductance, rotor inductance and mutual inductance respectively.  $\vec{v}_s$  is the stator voltage vector, which is obtained based on the selection of switching mode ( $S_a$ ,  $S_b$  and  $S_c$ ) from the relevant table [13].

$$\vec{v}_s (= [v_{sd} \ v_{sq}]^T) \quad (11)$$

Equation (12) is the stator current and (13) is the rotor current.

$$\vec{i}_s (= [i_{sd} \ i_{sq}]^T) \quad (12)$$

$$\vec{i}_r (= [i_{rd} \ i_{rq}]^T) \quad (13)$$

The meaning of the above equations is that the rotor flux depends on the stator flux with a first-order delay, which means that when the stator flux changes, the rotor flux can be considered constant and ignore its changes.

To put it more clearly, by selecting and applying the appropriate voltage vector, the stator flux can be changed and the angle between the rotor flux and the stator flux and as a result the motor torque can be controlled.

The crucial point here is choosing the right voltage vector for the control process. Assuming that the flux is in the first region we have [9]:

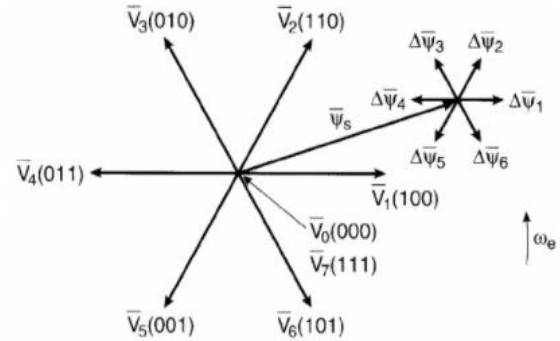

**Fig. 7. AN EXAMPLE OF HOW TO CHOOSE THE RIGHT VOLTAGE VECTOR FOR THE CONTROL PROCESS (ASSUMING THAT THE FLUX IS IN THE FIRST REGION)**

Figure 7 shows that by applying each of the 6 vectors shown, different torque and flux changes take place. For example, if the voltage vector  $V_3$  is applied, the torque will increase and the current will decrease.

As a general rule, it can be said that if the stator flux vector is in the m region, the application of the  $V_{m+2}$ ,  $V_{m-2}$ ,  $V_{m+3}$  vectors will decrease the flux, and the application of the  $V_{m-1}$ ,  $V_m$ ,  $V_{m+1}$  voltage vectors will increase the flux. Be made applying

vectors  $V_{m-1}$ ,  $V_{m-2}$  causes a decrease in torque, and applying vectors  $V_{m+1}$ ,  $V_{m+2}$  causes an increase in torque.  $V_m$ ,  $V_{m+3}$  vectors can decrease or increase the torque depending on the location of the joint. In Table 4, it is shown in summary that the selection and application of each of the voltage vectors has the following effect:

TABLE 4. THE EFFECT OF CHOOSING DIFFERENT VOLTAGE VECTORS ON MOTOR FLUX AND MOTOR TORQUE

Vector	$V_{n-2}$	$V_{n-1}$	$V_n$	$V_{n+1}$	$V_{n+2}$
Flux	decrease	increase	increase	increase	decrease
Torque	decrease	decrease	It depends	increase	increase

Hysteresis comparator is used in this control system. A two-level comparator is used for flux, and a three-level comparator is used for torque control (due to increased efficiency and reduced torque ripple). As explained below:

$$\Delta\psi_s = \begin{cases} 1 & \text{if } |\psi_s| \leq |\psi_s^*| - |Hysteresis\ Band| \\ 0 & \text{if } |\psi_s| \geq |\psi_s^*| + |Hysteresis\ Band| \end{cases} \quad (14)$$

$$\Delta T_e = \begin{cases} 1 & \text{if } T_e \leq T_e^* - |Hysteresis\ Band| \\ 0 & \text{if } T_e = T_e^* \\ -1 & \text{if } T_e \geq T_e^* + |Hysteresis\ Band| \end{cases} \quad (15)$$

## 2.1. Calculation of reference flux and torque

The reference current is usually set up to the nominal speed equal to the motor's nominal current (fixed value). After the nominal speed, we must weaken the stator current by so that the motor voltage does not exceed the nominal value. The size of the stator flux is approximately obtained from the following equation.  $V_{ph}$  is the voltage of the stator phase and  $f$  is the nominal frequency.

$$|\vec{\psi}_1^s| = \frac{L_1}{\sqrt{R_1^2 + (2\pi \cdot f \cdot L_1)^2}} \cdot \sqrt{2} V_{ph} \quad (16)$$

The reference torque is generated by the speed control loop. In this way, the speed of the motor is compared with the reference speed, and the appropriate reference torque is generated by a PI controller, in order to zero the error.

## 2.2. Introduction of the suggested method of flux adjustment

In the traditional DTC method, a nominal and fixed hysteresis band is always used during the operation, therefore the flux range is strongly affected at low

speeds. If we always use a small hysteresis band, the torque ripple will be extremely high and the switching frequency will also increase significantly, which will reduce the efficiency of the driver. To solve this problem, a method has recently been introduced in a study [13] in which variable torque hysteresis band is used. This method makes it possible to avoid the selection of unnecessary small hysteresis band and as a result reverse voltage vectors at medium and high speeds. Of course, the drawback of this method is that at a certain speed The critical speed (high and low band) are switched at the same time, which causes us to have a lot of overshoots in the torque due to the continuous switching of the active voltage vectors instead of the zero voltage vectors. Again, in this method, the torque ripple of the switching frequency is relatively high. In this paper, a small hysteresis band has been introduced, which is used at medium to high speed from the nominal hysteresis band, and at a certain speed, only one of the upper or lower bands is switched to the small hysteresis band. This method is focused on reducing the duration of the negative slope of the torque, which has caused the length of time to select zero voltage vectors to be reduced, and so on. Now the selection of reverse voltage vectors should also be minimized. In this method, due to maintaining the nominal hysteresis band at medium and high speeds, torque overshoots have been reduced well.

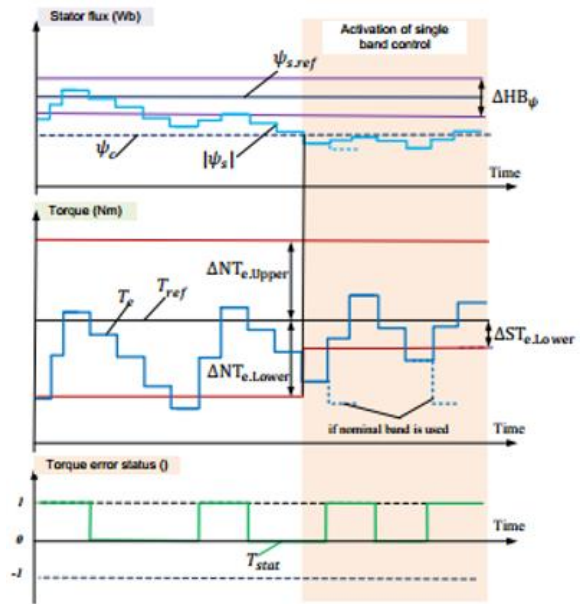


Fig. 8. SCHEMATIC OF THE STATOR FLUX, TORQUE AND TORQUE ERROR STATUS BY USING ONLY ONE BAND HYSTERESIS CONTROL OF THE FORWARD DIRECTION

Figure 8 shows that first, a critical flux point must be selected to determine the range of flux loss at low speeds. The speed corresponding to the critical flux point is also indicated by.

Nominal and small hysteresis bands are switched according to the following conditions:

$$HTB = \begin{cases} \Delta NT_{e.Upper} \text{ and } \Delta NT_{e.lower} & \omega_r > \omega_r^{\psi_c} \\ \Delta NT_{e.Upper} \text{ and } \Delta ST_{e.lower} & 0 \leq \omega_r < \omega_r^{\psi_c} \end{cases} \quad (17)$$

$$HTB = \begin{cases} \Delta ST_{e.Upper} \text{ and } \Delta NT_{e.lower} & -\omega_r^{\psi_c} \leq \omega_r < 0 \\ \Delta NT_{e.Upper} \text{ and } \Delta NT_{e.lower} & \omega_r < -\omega_r^{\psi_c} \end{cases} \quad (18)$$

It is clear that in 18, for speeds higher than the critical speed, both the upper and lower bands are nominal, but in the speed range between zero and the critical speed, the nominal upper band and the small lower band are selected. Equation 18 also states this condition for the opposite direction.

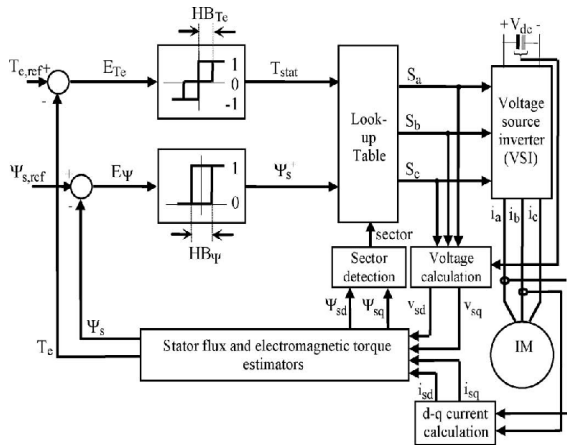


**Fig. 9. CONTROL DIAGRAM OF DTC INDUCTION MOTOR DRIVE BASED ON BAND HYSTERESIS WITH INTRODUCED CONTROL STRATEGY**

In this section, first, 3 different types of DTC method are simulated in MATLAB software, and then to prove the superiority of the proposed method of this study, the simulation results are compared. The specifications of the 3-phase induction motor as well as the DTC parameters used in these simulations are listed in the Table 5:

**TABLE 5. INDUCTION MOTOR AND DTC DRIVE PARAMETERS USED IN MATLAB SIMULATION**

Induction Motor Values			
3.7 kW	3.7 kW	3.7 kW	3.7 kW
8.28 A	8.28 A	8.28 A	8.28 A
1750 r/min	1750 r/min	1750 r/min	1750 r/min
20.36Nm	20.36Nm	20.36Nm	20.36Nm

0.6Wb	0.6Wb	0.6Wb	0.6Wb
Pole pairs		Pole pairs	
DTC Parameters			
DC Link Voltage		DC Link Voltage	
Torque hysteresis band(nominal)		Torque hysteresis band(nominal)	
Torque hysteresis band(small)		Torque hysteresis band(small)	
Flux hysteresis band		Flux hysteresis band	

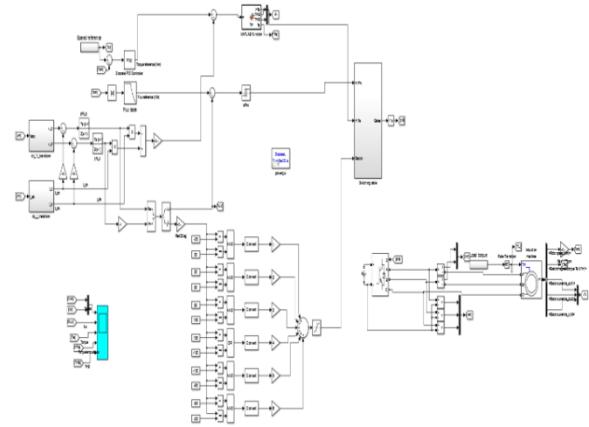


**Fig. 10. BLOCK DIAGRAM OF THE SIMULATION OF INDUCTION MOTOR AND INTRODUCED DRIVE METHOD**

In this paper, the bandwidth of the torque hysteresis in the normal state (nominal THB) is 2.5 Nm, which is about 10-15% of the nominal torque. Also, the hysteresis bandwidth of the small THB is 0.01 Nm, which is about 0.5% of the nominal torque. The number should be chosen small enough so that the duration of the negative slope of the torque does not increase, which leads to a long selection of zero voltage vectors.

In the following figures, the simulation results for speed, stator current, torque, torque error mode and upper and lower hysteresis bands for all 3 original DTC methods, DTC-HB1 (in this method both upper and lower bands are controlled simultaneously) and DTC-HB2 (our proposed method that controls only one of the bands) be is shown. The sampling rate in all 3 simulations is selected as 50 microseconds and the critical speed is experimentally considered to be 70 revolutions per minute. The important point is that the simulation was done under light load conditions, because in these conditions, the duration of the negative slope of the torque is longer, and these results make our simulation more robust.

First mode: speed change with the original DTC method [2]

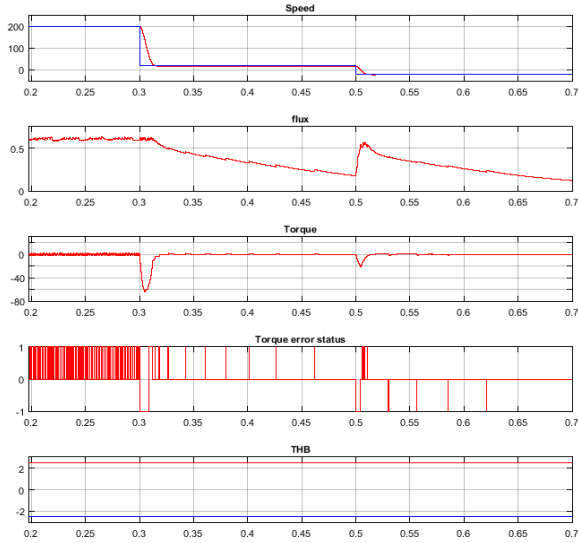


**Fig. 11.** SIMULATION RESULTS FOR THE ORIGINAL DTC DRIVE METHOD OF INDUCTION MOTORS AT 20 AND -20 RPM UNDER LIGHT LOAD

Figure 11 which is related to the conventional DTC, it is clear that at 200RPM the flow is stable and there are no problems. However, at 20RPM and -20RPM, which is less than the critical speed, the problem of current drop is clearly evident. This current drop also causes the speed and torque to fluctuate. Also, in this form, zero voltage vectors are injected for a long time. It is also clear that it originates from the long duration of the negative slope of the torque.

The second mode: speed change with the DTC-HB1 method [13]

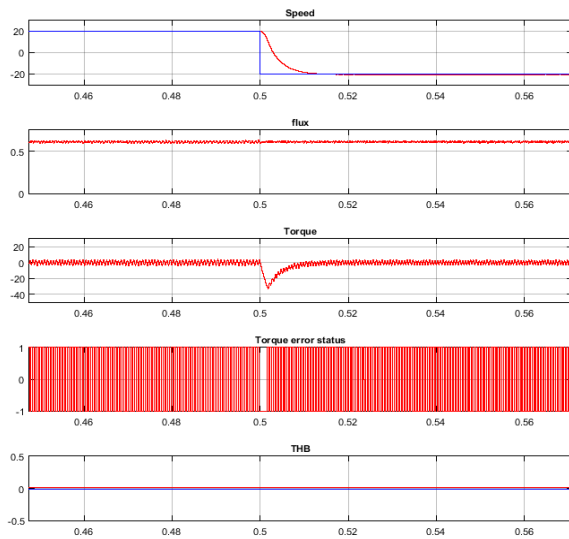


**Fig. 12.** SIMULATION RESULTS FOR THE DTC-HB1 DRIVE METHOD OF INDUCTION MOTORS AT 20 AND -20 RPM UNDER LIGHT LOAD

Figure 12 related to DTC-HB1 performance is shown at 20RPM and -20RPM speeds, which are lower than the critical speeds. In this case, the high and low bands are controlled at the same time, the flux is well stabilized and the flux loss defect in the first Figure has been resolved, but the switching frequency has increased greatly, and the torque ripple has also increased.

The third mode: speed change with the DTC-HB2 method (proposed method)

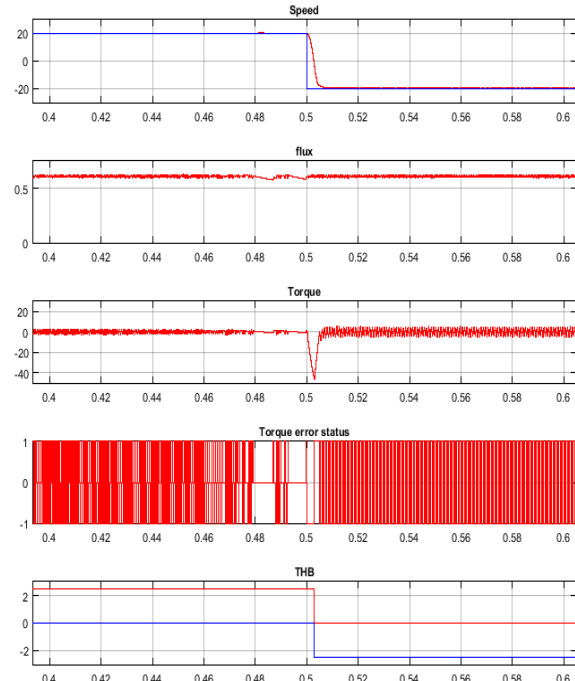


**Fig. 13.** SIMULATION RESULTS FOR DTC-HB2 DRIVE METHOD OF INDUCTION MOTORS AT RPM SPEEDS OF 20 AND -20 UNDER LIGHT LOAD

Figure13 also shows the performance of DTC-HB2 at 20RPM and -20RPM speeds, which are lower than the critical speeds.

### 3. CONCLUSIONS

In the proposed method of this study, according to the direction of rotation of the motor at speeds lower than the critical speed, only one of the upper or lower bands is controlled, which causes the torque ripple to decrease significantly while we have a stable flux, as well as the switching frequency. It can be clearly seen that not only the selection of zero voltage vectors has been minimized, but also the unnecessary switch of reverse voltage vectors has been avoided. This means increasing the efficiency and quality of the system while maintaining the simplicity of the structure.



## REFERENCES

- [1] Marulasiddappa HB, Pushparajesh V. Review on different control techniques for induction motor drive in electric vehicle. *IOP Conf Ser Mater Sci Eng.* 2021;1055(1):012142.
- [2] Faizal A, Miefthawati NP, Kurniawan R, Marzuki CC. Direct Torque Control Design with Fuzzy Sugeno-Proportional Derivative for 3-Phase Induction Motor Speed Control. 2023;10(1):111–20.
- [3] Maghfiroh H, Iftadi I, Sujono A. Speed Control of Induction Motor using LQG. *J Robot Control.* 2021;2(6).
- [4] Dianguo Xu, Bo Wang, G. Zhang, G. Wang, Young Yu. A Review of Sensorless Control Methods for AC Motor Drives. *Ces Trans Electr Mach Syst.* 2018;2(1):104–15.
- [5] Kohlrusz G, Fodor D. Comparison of Scalar and Vector Control Strategies of Induction Motors. *Hungarian J Ind Chem Veszprém.* 2011;39(2):265–70.
- [6] Tekam MS, Sharma DAK. Comparative Study of Field Oriented Control and Direct Torque Control of Induction Motor. *Int J Sci Dev Res [Internet].* 2018;3(7):209–17. Available from: [www.ijedr.org](http://www.ijedr.org)
- [7] A. B. Jidin, N. R. B. N. Idris, A. B. M. Yatim, M. E. Elbuluk, and T. Sutikno, "A Wide-Speed High Torque Capability Utilizing Overmodulation Strategy in DTC of Induction Machines With Constant Switching Frequency Controller," *IEEE Trans. Power Electronics*, vol. 27, no. 5, pp. 2566-2575, 2012.
- [8] J. N. Nash, "Direct torque control, induction motor vector control without an encoder," *IEEE Trans. Ind. Appl.*, vol. 33, no. 2, pp. 333-341, March/April 1997.
- [9] D. Mohan, X. Zhang and G. H. B. Foo, "Three-Level Inverter-Fed Direct Torque Control of IPMSM With Torque and Capacitor Voltage Ripple Reduction," *IEEE Trans. Energy Convers.*, vol. 31, no. 4, pp. 1559-1569, Dec. 2016.
- [10] Savarapu S, Qutubuddin M, Narri Y. Modified Brain Emotional Controller-Based Ripple Minimization for SVM-DTC of Sensorless Induction Motor Drive. *IEEE Access.* 2022;10:40872–87.
- [11] Yang Y, Wang Q, Shang J. Five-Level Hysteresis DTC of Open-End Winding Permanent Magnet Synchronous Motors with Zero-Sequence Currents Suppression and Torque Ripple Reduction. *IEEE Access.* 2022;10(October):121762–71.
- [12] Loncarski J, Monopoli VG, Leuzzi R, Cupertino F. Operation analysis and comparison of Multilevel Si IGBT and 2-level SiC MOSFET inverter-based high-speed drives with long power cable. *ICCEP 2019 - 7th Int Conf Clean Electr Power Renew Energy Resour Impact.* 2019;503–9.
- [13] I. M. Alsofyani, N. R. N. Idris, and Y. A. Alamri, "An improved flux regulation using a controlled hysteresis torque band for DTC of induction machines," in *Proc. IEEE Conf. Energy Convers.*, 2015, pp. 368-372.